ECS Journal of Solid State
Science and Technology

Pt/GaN Schottky Barrier Height Lowering by Incorporated Hydrogen

ECS Journal of Solid State Science and Technology, 2024 **13** 045002

Pt/GaN Schottky Barrier Height Lowering by Incorporated Hydrogen

Yoshihiro Irokawa,[z] Akihiko Ohi, Toshihide Nabatame, and Yasuo Koide

National Institute for Materials Science, Tsukuba, Ibaraki 305-0044, Japan

Changes in the hydrogen-induced Schottky barrier height (Φ_B) of Pt/GaN rectifiers fabricated on free-standing GaN substrates were investigated using current–voltage, capacitance–voltage, impedance spectroscopy, and current–time measurements. Ambient hydrogen lowered the Φ_B and reduced the resistance of the semiconductor space–charge region while only weakly affecting the ideality factor, carrier concentration, and capacitance of the semiconductor space–charge region. The changes in the Φ_B were reversible; specifically, the decrease in Φ_B upon hydrogen exposure occurred quickly, but the recovery was slow. The results also showed that exposure to dry air and/or the application of a reverse bias to the Schottky electrodes accelerated the reversion compared with the case without the applied bias. The former case resulted in fast reversion because of the catalytic effect of Pt. The latter case, by contrast, suggested that hydrogen was incorporated into the Pt/GaN interface oxides as positive mobile charges. Moreover, both exposure to dry air and the application of a reverse bias increased the Φ_B of an as-loaded sample from 0.91 to 1.07 eV, revealing that the Φ_B of Pt/GaN rectifiers was kept lower as a result of hydrogen incorporation that likely occurred during device processing and/or storage.

 [DOI: 10.1149/2162-8777/ad3959]

Manuscript received March 17, 2024. Published April 9, 2024.

Gallium nitride (GaN) has been extensively used in optical and electronic devices because of its advantages,[1] which include a wide (3.4 eV) direct bandgap, easy fabrication of heterostructures using nitride-based materials such as AlGaN and InGaN, and a high saturation velocity (e.g., 1.9×10^7 cm s^{-1} at a sheet charge density of 7.8×10^{11} cm^{-2} at room temperature).[2] As the commercialization of high-quality free-standing bulk GaN substrates proceeds, researchers are dramatically improving the performance of GaN electronic devices by exploiting the advantages of substrates with a low dislocation density; consequently, a wide variety of GaN-based devices, including Schottky barrier diodes (SBDs),[3] *p–n* junction diodes,[4] junction-barrier Schottky diodes,[4,5] and metal-oxide-semiconductor field-effect transistors (MOSFETs),[3,6,7] have recently attracted much attention. Nonetheless, knowledge of the reliability of these devices remains limited and little is known about the suitability of these devices for use in real electronic structures such as power conversion systems. Among factors affecting the device reliability, hydrogen incorporation into devices can cause serious complications in device characteristics because hydrogen ubiquitously exists in semiconductor processing and in the storage environment and easily penetrates into the device materials, changing the device characteristics unintentionally.[8–11] In the case of MOSFETs, the effects of ambient hydrogen on Si and SiC devices have long been studied; hydrogen-induced dipole layers have been proposed to be the primary factor leading to changes in the threshold voltages of these devices.[12] With respect to GaN metal-oxide-semiconductor (MOS) capacitors, by contrast, we recently reported that ambient hydrogen was incorporated into dielectric layers as positively charged mobile ions, leading to flatband voltage shifts of the devices.[13] In that report, we revealed that oxide layers in MOS devices played a critical role in the flatband voltage shifts; that is, we speculated that the flatband voltage shifts originated from trapped hydrogen at oxygen vacancies (V_Os) in the oxide layers.[13] In addition, even for GaN SBDs, we found that the formation of oxides at the Pt/GaN interface might be responsible for the reduction of the Schottky barrier height (Φ_B) as a result of hydrogen exposure.[14,15] That is, we hypothesized that hydrogen trapped at V_Os in the Pt/GaN interface oxide changed the resistivity of the oxide layers, resulting in the Φ_B reductions.

In our previous study involving GaN MOS capacitors, the application of a reverse gate bias during the reversion revealed the charging state of hydrogen in the oxide layers.[13] For GaN SBDs, however, the charging state of hydrogen is unknown. In the present study, we used current–voltage (*I–V*), capacitance–voltage (*C–V*), impedance spectroscopy, and current–time (*I–t*) measurements to investigate the charging state, along with the hydrogen response and reversion characteristics, of Pt/GaN SBDs. As a result, we found that hydrogen can be incorporated into the native oxide at the Pt/GaN interfaces as positive mobile charges, as previously observed in GaN MOS capacitors. In addition, we found that the Φ_B of Pt/GaN rectifiers is kept lower because of the hydrogen incorporation at the Pt/GaN interface oxides, which likely occurs during device processing and/or storage, where the incorporated hydrogen does not desorb under conventional conditions such as room temperature and humid ambient air.

Experimental

Figure 1 shows a schematic cross-section of the Pt/GaN SBD structure investigated in the present study. The devices were prepared as follows: 5 μm-thick GaN layers were epitaxially grown on free-standing bulk n^+-GaN(0001) substrates via metal-organic vapor-phase epitaxy. The grown GaN layers were doped with Si at a concentration of 2×10^{16} cm^{-3}, and the substrates had a dislocation density on the order of approximately 10^6 cm^{-2} and a carrier concentration of 1×10^{18} cm^{-3}. After the surface was cleaned with a mixture of sulfuric acid and hydrogen peroxide (H_2SO_4:H_2O_2 = 1:1) to remove organic residues, Ti (20 nm)/Al (100 nm)/Pt (40 nm)/Au (100 nm) back Ohmic contacts were patterned via electron-beam deposition. The patterned substrates were then annealed at 750 °C for 30 s under a flowing N_2 atmosphere in a rapid thermal annealing system. After formation of the Ohmic contacts, circular Pt (25 nm) Schottky contacts with a diameter of 100 μm were formed through a lift-off process. Notably, we confirmed that this surface cleaning method led to the generation of crystalline native gallium oxide layers with a thickness of ~1 nm on their surfaces; the in-plane lattice constant of the oxide matched that of GaN.[16,17]

The reaction of the fabricated devices to ambient hydrogen gas was studied at room temperature in a stainless-steel chamber equipped with tungsten probes. After the chamber was evacuated by a dry scroll vacuum pump, flowing pure N_2 gas was introduced at a rate of 100 mL min^{-1} and a total pressure of 10.0 kPa; *I–V*, *C–V*, and impedance spectroscopy measurements were then conducted under pure N_2 gas. Next, in place of pure N_2 gas, flowing 1% H_2 + N_2

[z]E-mail: IROKAWA.Yoshihiro@nims.go.jp

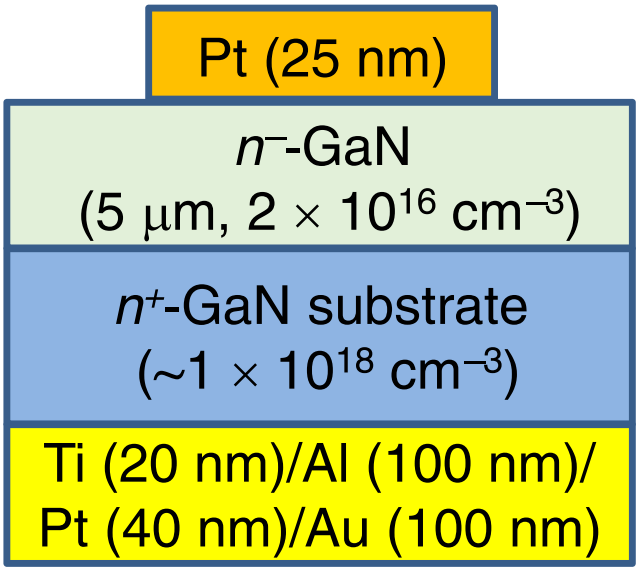

Figure 1. Schematic of Pt/GaN SBD structure investigated in the present study.

mixture gas was introduced at the same flow rate and same total pressure and the devices in pure N_2 gas were measured using the same methods after saturation of the device characteristics. For some devices, the hydrogen reaction transient was also recorded using the *I–t* method. Finally, the flowing gas was changed from 1% H_2 + N_2 mixture gas to either pure N_2 gas or dry air gas at the same flow rate and same total pressure; the recovery transients for some of the devices were then measured using the *I–t* technique. All the *I–V* and *C–V* measurements were performed with a delay time of 1 s, and the frequency of the *C–V* measurements was 100 kHz.

Results and Discussion

Figure 2 shows the *I–V* characteristics for a Pt/GaN SBD in pure N_2 gas and their changes when the device was exposed to the 1% H_2 + N_2 mixture gas. The SBD displayed an excellent on/off ratio under both environments; the current in the device under the 1% H_2 + N_2 mixture gas was enhanced compared with that in the device under pure N_2 gas, consistent with previous reports.[14,15,18] In Fig. 2, the current in the SBD under ambient H_2 gas is approximately 10^4 times greater than that in the device under pure N_2 gas. This current gain was previously explained by the dipole model in which the apparent Φ_B reduction originated from the hydrogen-induced dipole layer formed at the metal/semiconductor interfaces;[12,19] however, we have proposed a different model in which hydrogen induces changes in the Pt/GaN interface oxide properties, resulting in the observed increases in current in the devices under an ambient hydrogen atmosphere.[14,15] The ideality factor (n) and Schottky barrier height determined from *I–V* characteristics (Φ_B') were calculated from the forward *I–V* curves on the basis of the thermionic emission theory (Table I).[20] We then conducted *C–V* measurements to compare the net donor concentration $N_D - N_A$ of GaN under pure N_2 gas with that of GaN under 1% H_2 + N_2 mixture gas, where N_D and N_A are the donor and acceptor densities, respectively.

Figure 3 shows the $1/C^2$ versus V data obtained from the *C–V* characteristics for a Pt/GaN SBD under pure N_2 gas and their changes when the device was exposed to 1% H_2 + N_2 mixture gas. As shown in Fig. 3, all the data are plotted on two parallel straight lines with different intercepts; that is, the line corresponding to the data for the device under the 1% H_2 + N_2 mixture gas has a smaller intercept than the line corresponding to the data for the device under pure N_2 gas, as we previously reported.[14,15] The results in Fig. 3 suggest the following two points: First, the $N_D - N_A$ of the Pt/GaN SBD under 1% H_2 + N_2 mixture gas is the same as that under pure N_2 gas because the two lines have the same slope.[20] Second, the Schottky barrier height determined from the *C–V* characteristics (Φ_B'') of the Pt/GaN SBD under 1% H_2 + N_2 mixture gas is smaller than that of the device under pure N_2 gas.[20] We calculated the $N_D - N_A$ and Φ_B'' values on the basis of the data in Fig. 3; the results are reported in Table I, together with the n and Φ_B' values acquired from Fig. 2.

The values in Table I are similar to those reported in our previous paper except for the Φ_B' and Φ_B'' values for the Pt/GaN SBD under pure N_2;[15] the reason for this discrepancy is discussed later. As noted in our previous paper,[15] the data in Table I suggest the following three issues: First, both the Φ_B' and Φ_B'' values for the Pt/GaN SBD under 1% H_2 + N_2 mixture gas are lower than those for the device under pure N_2 gas; we assume that changes in the Pt/GaN interface oxide properties brought about by hydrogen reduce the Φ_B' and Φ_B'' values. Second, the $N_D - N_A$ value for the Pt/GaN SBD under 1% H_2 + N_2 mixture gas is the same as that for the device under pure N_2 gas, as evidenced by the two parallel $1/C^2$ vs V curves in Fig. 3; this value is roughly consistent with the doping concentration of Si into GaN. Thus, hydrogen does not alter the electrical properties of the GaN layers, implying that hydrogen instead changes the Pt/GaN interface oxide properties. Third, the n does not change after the device is exposed to 1% H_2 + N_2 mixture gas, meaning that the current transport mechanism is the same under both of the investigated ambient environments. Next, we used impedance spectroscopy to investigate whether the previously proposed hydrogen-induced dipole layer exists.

Figure 4 shows Nyquist plots for a Pt/GaN SBD at 0 V in pure N_2 gas and in 1% H_2 + N_2 mixture gas. The result is consistent with our previous report in which hydrogen exposure was found to result in a

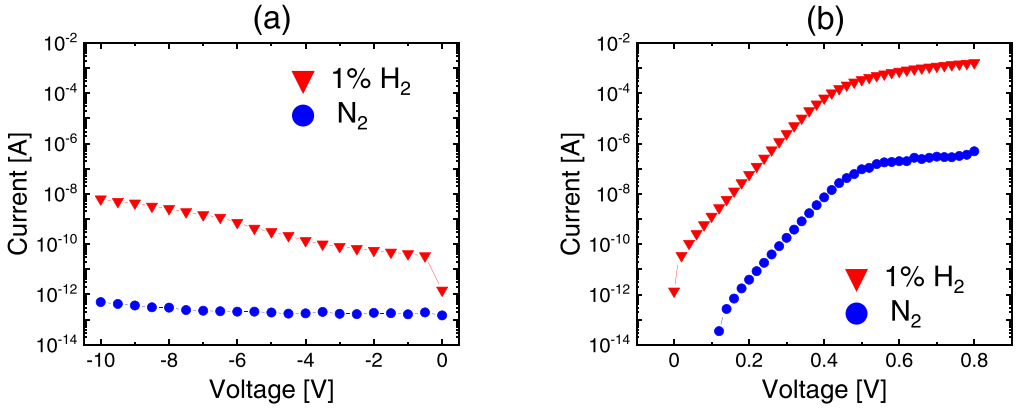

Figure 2. *I–V* characteristics for a Pt/GaN SBD in pure N_2 and the changes of the characteristics when the devices were exposed to 1% H_2 + N_2. Here, blue circles represent data corresponding to pure N_2 gas and red inverted triangles represent data corresponding to 1% H_2 + N_2 mixture gas.

Table I. Summary of n and Φ_B' values obtained from the data in Fig. 2 and the $N_D - N_A$ and Φ_B'' values based on the data in Fig. 3.

Property	Value under pure N_2	Value under 1% H_2 + N_2
n	1.02	1.02
Φ_B'	1.01	0.76
$N_D - N_A$	2.3×10^{16}	2.3×10^{16}
Φ_B''	1.22	0.86

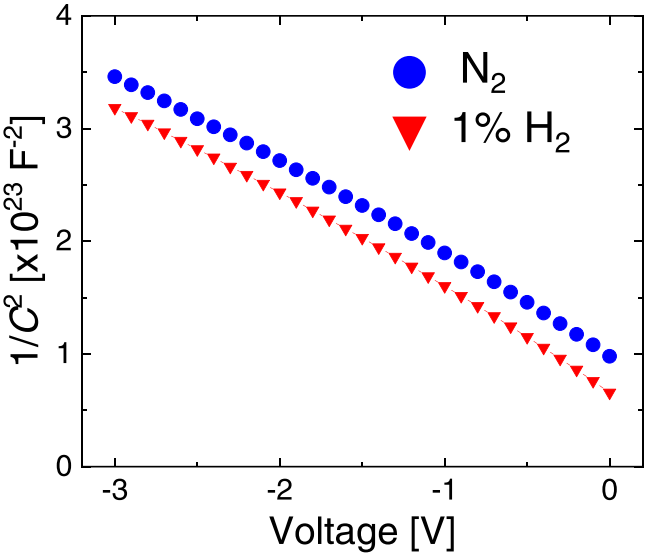

Figure 3. $1/C^2$ vs V curves for a Pt/GaN SBD under pure N_2 and their changes when the device was exposed to 1% H_2 + N_2. Here, blue circles represent data corresponding to pure N_2 gas and red inverted triangles represent data corresponding to 1% H_2 + N_2 mixture gas.

striking reduction of the radius of the semicircle in the Nyquist plot;[14,15] these semicircle shapes can be explained according to equivalent RC parallel circuits representing the semiconductor space–charge region, where R and C are the resistance and capacitance of the semiconductor space–charge region, respectively.

Table II shows the R and C values calculated from the Nyquist plots in Fig. 4. As reported previously,[14,15] exposure to hydrogen drastically reduced the R value: the R value for a Pt/GaN SBD in 1% H_2 + N_2 mixture gas was approximately 10^4 times smaller than that of the device under pure N_2 gas, whereas the C value remained almost constant. We assume that this result is attributable to hydrogen-induced reduction of the Pt/GaN interface oxide resistance for the following three reasons: First, as shown in Fig. 4b, a new semicircle attributable to the hydrogen-induced dipole layer is not observed after the Pt/GaN SBD was exposed to hydrogen; therefore, the previously proposed model does not appear to justify the data. Second, as discussed previously (Fig. 3 and Table I), the $N_D - N_A$ value for the Pt/GaN SBD in 1% H_2 + N_2 mixture gas is the same as that for the device in pure N_2 gas; therefore, hydrogen exposure does not change the electrical properties of the GaN layers. According to our previous study involving GaN MOS capacitors,[13] oxide layers between Pt and GaN are the most likely origin of the change in the Pt/GaN interface oxide resistance because hydrogen was found to be absorbed into the oxide layers as positive mobile charges. Third, hydrogen-induced property changes in oxides have been reported for various oxides, including TiO_2,[21] Ta_2O_5,[22] HfO_2,[23] $Pb(Zr,Ti)O_3$,[24] $SrBi_2Ta_2O_9$,[25] $SrTiO_3$,[26] and $BaTiO_3$;[27] hydrogen is known to reduce the resistance of these oxides. Hydrogen is ionized in the oxides, and electrons emitted from hydrogen contribute to the lowering of the resistance.[24,26,28] We assume that the same phenomenon occurs in the Pt/GaN interface oxide. We subsequently investigated the reaction timeframe of a Pt/GaN SBD under a hydrogen ambient atmosphere.

Figure 5 shows the current for a Pt/GaN SBD at 0.15 V as a function of time after the sample was exposed to 1% H_2 + N_2 mixture gas. As shown in Fig. 5, the current drastically increases after hydrogen exposure and saturates at $\sim 10^{-8}$ A within a few minutes; therefore, we recorded all of the data for the devices under 1% H_2 + N_2 mixture gas (Figs. 2–4, and 8) after 30 min of exposure so that the hydrogen reaction had completed. Note that the saturation time for the Pt/GaN SBD is within the same timeframe as that for previously reported GaN MOS capacitors.[13] Next, we investigated the recovery characteristics of a Pt/GaN SBD after hydrogen reaction.

Figure 6 shows the recovery characteristics for a Pt/GaN SBD. Note that the current at 0 min is the value in 1% H_2 + N_2 mixture gas after saturation (Fig. 5). When the ambient atmosphere was changed from hydrogen to either pure N_2 gas or dry air gas, the current gradually reverted to its initial value observed under pure N_2 gas. Figure 6 shows that the nature of the ambient gas plays a critical role in the recovery velocity; that is, dry air gas leads to a much faster recovery than pure N_2 gas, consistent with our previously reported results.[14,15] This fast recovery under ambient dry air gas is attributable to the catalytic function of Pt in which hydrogen and oxygen chemically react on Pt surfaces, resulting in rapid desorption of hydrogen from the Pt/GaN interface oxides, as previously reported.[29,30] Next, we investigated the effect of applying a reverse bias during the reversion in order to reveal the charging state of hydrogen in oxide layers and to compare the effect of the ambient atmosphere and the bias application on the recovery rate.

Figure 7 shows the recovery characteristics for a Pt/GaN SBD, where the reversion after hydrogen exposure was compared between an SBD under pure N_2 gas and an SBD under pure N_2 gas with a reverse bias of −2 V applied. Note that the measurements were

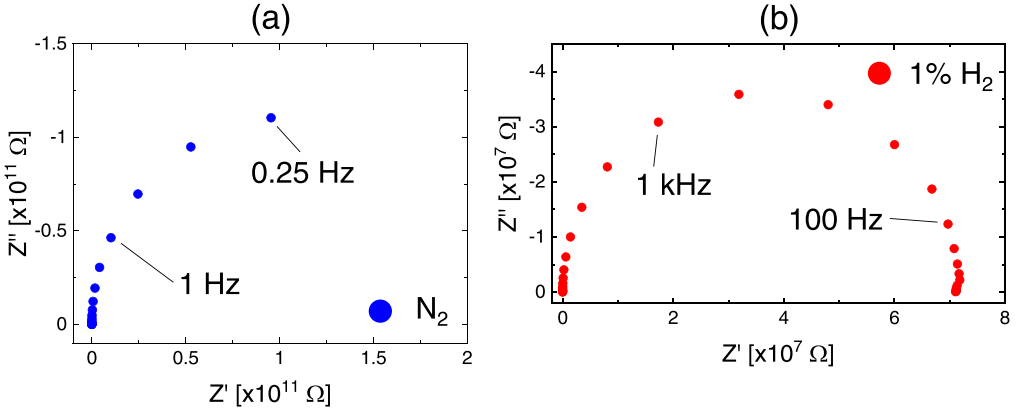

Figure 4. Nyquist plots for a Pt/GaN SBD at 0 V (a) under pure N_2 gas and (b) under 1% H_2 + N_2 mixture gas.

Table II. Summary of *R* and *C* values extracted from the Nyquist plots in Fig. 4.

Parameter	Value under pure N_2	Value under 1% H_2 + N_2
R [Ω]	2.2×10^{11}	7.2×10^{7}
C [pF]	3.2	3.9

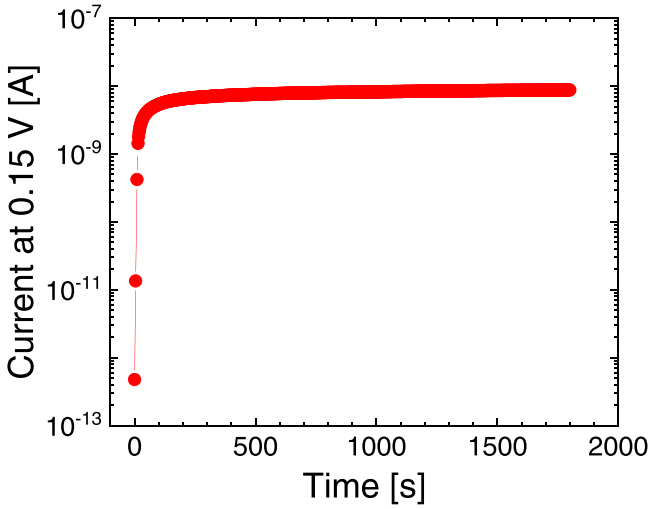

Figure 5. Current at 0.15 V for a Pt/GaN SBD, plotted as a function of time after exposure to hydrogen.

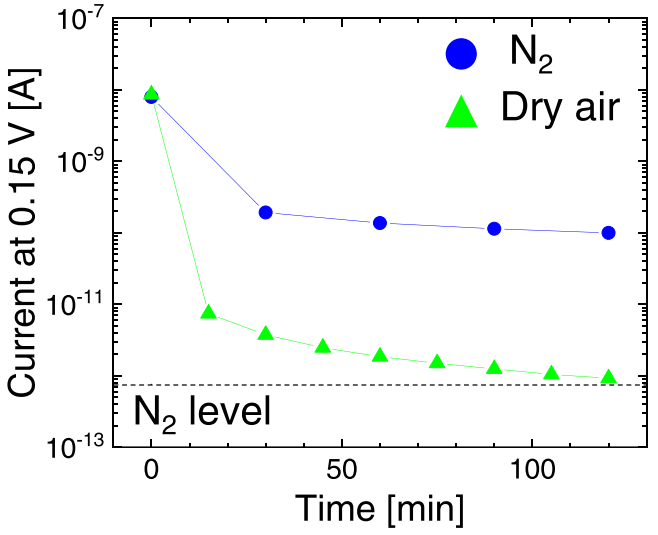

Figure 6. Recovery characteristics for a Pt/GaN SBD. Here, blue circles and green triangles represent data corresponding to pure N_2 and data corresponding to dry air, respectively.

performed six times in total for three different devices; the standard errors are shown as the error bars with the mean values.[31] We previously reported that applying a reverse gate bias accelerated the reversion of GaN MOS capacitors with Al_2O_3 and $Hf_{0.57}Si_{0.43}O_x$ gate dielectrics after hydrogen exposure.[13,29] We explained this acceleration as follows:[13,29] Hydrogen absorbed into the dielectrics as positive mobile charges, and these mobile charges were driven toward the gate electrodes by the applied electric field, leading to faster hydrogen desorption. In the case of a Pt/GaN SBD, ∼1 nm-thick crystalline native gallium oxide layers exist at the Pt/GaN interfaces, as described earlier, instead of gate dielectrics; we assume

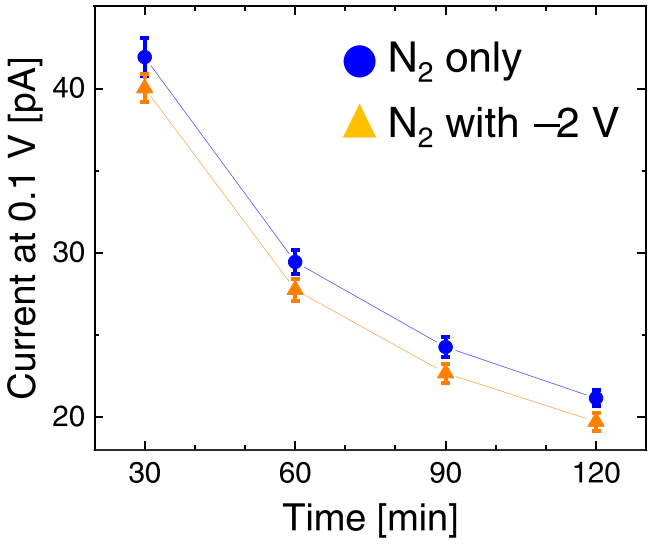

Figure 7. Recovery characteristics for a Pt/GaN SBD. Here, blue circles represent data corresponding to pure N_2 and orange triangles represent data corresponding to pure N_2 under a reverse bias of −2 V. Measurements were performed six times in total for three different devices; the standard errors are shown as the error bars with the mean values.

that hydrogen absorbed into the native gallium oxide layers induced the property changes in the Pt/GaN interface oxides. As shown in Fig. 7, the application of a −2 V bias slightly enhanced the restoration of the device, suggesting that hydrogen can be absorbed into the interface oxide layers as positive mobile charges, as in the oxides of MOS devices.[13,29] However, the effect of the bias application is less prominent than in the case of the MOS devices. A possible reason for this difference might be that an electric field sufficiently strong to desorb hydrogen was not applied to the oxide, likely because of the poor quality of the oxide at the Pt/GaN interfaces.[17] As a result, changing the ambient atmosphere is found to be much more effective for faster restoration. Next, we studied the changes in the Φ_B' values of as-loaded samples using the hydrogen desorption method developed here.

Figure 8 shows forward *I*–*V* characteristics for a Pt/GaN SBD in the as-loaded condition, as measured in vacuum, and the changes in the characteristics when the device was exposed to either 1% H_2 + N_2 mixture gas or dry air gas under a reverse bias of −2 V. The Φ_B' values were calculated on the basis of thermionic emission theory for each case. As shown in Fig. 8, the as-loaded Pt/GaN SBD has a Φ_B' value of 0.91 eV, consistent with our previously reported results.[14,15] Note that the Φ_B' value of a Pt/GaN SBD in the as-loaded condition maintained a similar value when the ambient atmosphere was changed from vacuum to pure N_2 gas. The key issue that emerges from Fig. 8 is that exposing the device to dry air gas under a reverse bias of −2 V increased the Φ_B' substantially compared with the Φ_B' under the as-loaded condition. As shown in Fig. 8, the as-loaded Pt/GaN SBD has a Φ_B' value of 0.91 eV; thereafter, the Φ_B' value increases to 1.07 eV as incorporated hydrogen desorbs under the dry air gas ambient atmosphere and applied bias, suggesting that hydrogen was already absorbed into the Pt/GaN interface oxide layers to some extent before the experiment, likely during processing and/or storage. We previously studied the hydrogen interaction of GaN MOS capacitors with various oxides, revealing that the number of V_Os in oxides might be related to hydrogen absorption.[13] In the case of a Pt/GaN SBD, hydrogen might be trapped at V_Os in the oxide layers because these oxides were found to be defective in our previous study.[17] The data in Fig. 8 show that the Φ_B' varies in the range 0.76–1.07 eV depending on the amount of absorbed hydrogen and that this fluctuation range of Φ_B' can depend on the quality of the Pt/GaN interface oxides. Therefore, this method can be a useful

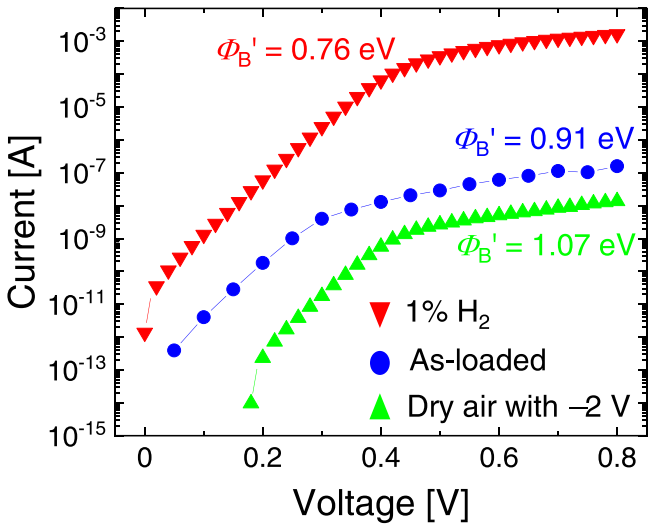

Figure 8. Forward *I–V* characteristics for a Pt/GaN SBD in the as-loaded condition, as measured in vacuum, and changes in the characteristics when the device is exposed to either 1% $H_2 + N_2$ or dry air under a reverse bias of −2 V. Here, blue circles represent data corresponding to the as-loaded condition in vacuum, red inverted triangles represent data corresponding to 1% $H_2 + N_2$, and green triangles represent data corresponding to dry air under a reverse bias of −2 V. The Φ_B' values were calculated on the basis of thermionic emission theory in each case.

tool to evaluate Pt/GaN interface oxides. Moreover, as shown in Table I, the Φ_B' and Φ_B'' values of Pt/GaN SBDs in pure N_2 gas are slightly higher than those in our previous reports (typically approximately $0.93 \leqslant \Phi_B' \leqslant 0.95$ and $1.17 \leqslant \Phi_B'' \leqslant 1.19$) [14,15] because the device was exposed to dry air gas before the Φ_B' and Φ_B'' measurements in the experiment; thus, the interface oxide lacked hydrogen compared with that in the device in the as-loaded condition. That is, the exact determination of Φ_B is generally not easy because of the nature of the incorporated hydrogen. Reported Φ_B' values of Pt/GaN SBDs, for instance, are largely scattered ($0.65 \leqslant \Phi_B' \leqslant 1.43$),[32–53] which might be related to the incorporated hydrogen.

Conclusions

Hydrogen-induced Φ_B changes of Pt/GaN SBDs fabricated on free-standing GaN substrates were investigated using *I–V*, *C–V*, impedance spectroscopy, and *I–t* measurements. Ambient hydrogen was found to lower the Φ_B and reduce the R while only weakly affecting the n, $N_D - N_A$, and C values; these results might be attributable to changes in the properties of the Pt/GaN interface oxides as a result of hydrogen absorption. The changes in the Φ_B values were reversible; specifically, the Φ_B values rapidly decreased upon exposure of the Pt/GaN SBDs to hydrogen; however, the recovery was slow. The application of a reverse bias to the Schottky electrodes accelerated the reversion compared with the case without a reverse bias, suggesting that hydrogen was absorbed into the oxides as positive mobile charges. In addition, both exposure to dry air and the application of a reverse bias were found to increase the Φ_B' value of the as-loaded sample from 0.91 to 1.07 eV, revealing that the Φ_B value of Pt/GaN rectifiers was kept lower as a result of hydrogen incorporation that likely occurred during processing and/or storage. The crystal quality of the Pt/GaN interface oxides might be related to the amount of absorbed hydrogen, and the method described in this report might be a useful tool for evaluating the interface oxide quality.

Acknowledgments

This research was supported in part by JSPS KAKENHI Grant Numbers 23K03949. The authors are also grateful to the members of the nanofabrication facility at the National Institute for Materials Science.

ORCID

Yoshihiro Irokawa https://orcid.org/0000-0002-6531-4356

References

1. T. Kachi, *Jpn. J. Appl. Phys.*, **53**, 100210 (2014).
2. S. Bajaj, O. F. Shoron, P. S. Park, S. Krishnamoorthy, F. Akyol, T. H. Hung, S. Reza, E. M. Chumbes, J. Khurgin, and S. Rajan, *Appl. Phys. Lett.*, **107**, 153504 (2015).
3. T. Oka, *Jpn. J. Appl. Phys.*, **58**, SB0805 (2019).
4. S. R. Stein et al., *IEEE Trans. Electron Devices (Early Access)*, **71**, 1494 (2024).
5. M. Matys, K. Kitagawa, T. Narita, T. Uesugi, J. Suda, and T. Kachi, *Appl. Phys. Lett.*, **121**, 203507 (2022).
6. Y. Ichikawa, K. Ueno, T. Kondo, R. Tanaka, S. Takashima, and J. Suda, *Jpn. J. Appl. Phys.*, **63**, 02SP31 (2024).
7. K. Ito, S. Iwasaki, K. Tomita, E. Kano, N. Ikarashi, K. Kataoka, D. Kikuta, and T. Narita, *Appl. Phys. Express*, **16**, 074002 (2023).
8. S. J. Pearton, J. W. Corbett, and M. Stavola, *Hydrogen in Crystalline Semiconductors* (Springer, Berlin) (1992).
9. J. I. Pankove and N. M. Johnson, *Hydrogen in Semiconductors* (Academic, New York) (1991).
10. N. H. Nickel, *Hydrogen in Semiconductors II* (Academic, New York) (1999).
11. S. J. Pearton, F. Ren, Y. L. Wang, B. H. Chu, K. H. Chen, C. Y. Chang, W. Lim, J. Lin, and D. P. Norton, *Prog. Mater Sci.*, **55**, 1 (2010).
12. I. Lundström, H. Sundgren, F. Winquist, M. Eriksson, C. K. Rülcker, and A. L. Spetz, *Sens. Actuators B*, **121**, 247 (2007).
13. Y. Irokawa, M. Inoue, T. Nabatame, and Y. Koide, *ECS J. Solid State Sci. Technol.*, **11**, 085010 (2022).
14. Y. Irokawa, *Jpn. J. Appl. Phys.*, **59**, 120901 (2020).
15. Y. Irokawa, T. Ohki, T. Nabatame, and Y. Koide, *Jpn. J. Appl. Phys.*, **60**, 068003 (2021).
16. Y. Irokawa, T. T. Suzuki, K. Yuge, A. Ohi, T. Nabatame, K. Kimoto, T. Ohnishi, K. Mitsuishi, and Y. Koide, *Jpn. J. Appl. Phys.*, **56**, 128004 (2017).
17. Y. Irokawa, K. Mitsuishi, T. T. Suzuki, K. Yuge, A. Ohi, T. Nabatame, T. Ohnishi, K. Kimoto, and Y. Koide, *Jpn. J. Appl. Phys.*, **57**, 098003 (2018).
18. B. P. Luther, S. D. Wolter, and S. E. Mohney, *Sens. Actuators*, **B56**, 164 (1999).
19. S. M. Sze and K. K. Ng, *Physics of Semiconductor Devices* (Wiley, New York) (2007).
20. D. K. Schroder, *Semiconductor Material and Device Characterization* (Wiley, New York) (2006).
21. W. P. Chen, Y. Wang, J. Y. Dai, S. G. Lu, X. X. Wang, P. F. Lee, H. L. W. Chan, and C. L. Choy, *Appl. Phys. Lett.*, **84**, 103 (2004).
22. L. Goux, J. Y. Kim, B. M. Kope, Y. Nishi, A. Redolfi, and M. Jurczak, *J. Appl. Phys.*, **117**, 124501 (2015).
23. S. Kim, D. Lee, J. Park, S. Jung, W. Lee, J. Shin, J. Woo, G. Choi, and H. Hwang, *Nanotechnology*, **23**, 325702 (2012).
24. A. Shafiei, C. Oprea, A. Alfantazi, and T. Troczynski, *J. Appl. Phys.*, **109**, 114108 (2015).
25. J. P. Han and T. P. Ma, *Appl. Phys. Lett.*, **71**, 1267 (1997).
26. Z. J. Shen, W. P. Chena, K. Zhu, Y. Zhuang, Y. M. Hu, Y. Wang, and H. L. W. Chan, *Ceram. Int.*, **35**, 953 (2009).
27. D. S. B. Heidary, W. Qu, and C. A. Randall, *J. Appl. Phys.*, **117**, 124104 (2015).
28. R. Hempelmann, *Physica B*, **226**, 72 (1996).
29. Y. Irokawa, T. Nabatame, A. Ohi, N. Ikeda, O. Sakata, and Y. Koide, *Jpn. J. Appl. Phys.*, **58**, 100915 (2019).
30. L. G. Petersson, H. M. Dannetun, and I. Lundström, *Phys. Rev. Lett.*, **52**, 1806 (1984).
31. G. Cumming, F. Fidler, and D. L. Vaux, *J. Cell Biol.*, **177**, 7 (2007).
32. K. Suzue, S. N. Mohammad, Z. F. Fan, W. Kim, O. Aktas, A. E. Botchkarev, and H. Morkoç, *J. Appl. Phys.*, **80**, 4467 (1996).
33. L. Wang, M. I. Nathan, T. H. Lim, M. A. Khan, and Q. Chen, *Appl. Phys. Lett.*, **68**, 1267 (1996).
34. H. Hasegawa, Y. Koyama, and T. Hashizume, *Jpn. J. Appl. Phys.*, **38**, 2634 (1999).
35. U. Karrer, O. Ambacher, and M. Stutzmann, *Appl. Phys. Lett.*, **77**, 2012 (2000).
36. J. M. DeLucca, S. E. Mohney, F. D. Auret, and S. A. Goodman, *J. Appl. Phys.*, **88**, 2593 (2000).
37. Y. Kokubun, T. Seto, and S. Nakagomi, *Jpn. J. Appl. Phys.*, **40**, L663 (2001).
38. K. M. Tracy, P. J. Hartlieb, S. Einfeldt, R. F. Davis, E. H. Hurt, and R. J. Nemanich, *J. Appl. Phys.*, **94**, 3939 (2003).
39. J. K. Kim, H. W. Jang, and J. L. Lee, *J. Appl. Phys.*, **94**, 7201 (2003).
40. O. Weidemann, E. Monroy, E. Hahn, M. Stutzmann, and M. Eickhoff, *Appl. Phys. Lett.*, **86**, 083507 (2005).
41. H. G. Kim, S. H. Kim, P. Deb, and T. Sands, *J. Electron. Mater.*, **35**, 107 (2006).
42. Y. Zhou, M. Li, D. Wang, C. Ahyi, C. C. Tin, J. Williams, M. Park, N. M. Williams, and A. Hanser, *Appl. Phys. Lett.*, **88**, 113509 (2006).
43. O. Cojocari and H. L. Hartnagel, *J. Vac. Sci. Technol. B*, **24**, 2544 (2006).
44. M. Ali, V. Cimalla, V. Lebedev, H. Romanus, V. Tilak, D. Merfeld, P. Sandvik, and O. Ambacher, *Sens. Actuators B*, **113**, 797 (2006).
45. Y. Irokawa, Y. Sakuma, and T. Sekiguchi, *Jpn. J. Appl. Phys.*, **46**, 7714 (2007).
46. F. Iucolano, F. Roccaforte, F. Giannazzo, and V. Raineri, *Appl. Phys. Lett.*, **90**, 092119 (2007).

47. F. Iucolano, F. Roccaforte, F. Giannazzo, and V. Raineri, *J. Appl. Phys.*, **102**, 113701 (2007).
48. H. Okada, A. Naruse, Y. Furukawa, and A. Wakahara, *Jpn. J. Appl. Phys.*, **50**, 01AD08 (2011).
49. H. Fu, X. Huang, H. Chen, Z. Lu, I. Baranowski, and Y. Zhao, *Appl. Phys. Lett.*, **111**, 152102 (2007).
50. A. Kumar, J. Dhillon, S. Verma, P. Kumar, K. Asokan, and D. Kanjilal, *Semicond. Sci. Technol.*, **33**, 085008 (2018).
51. H. Imadate, T. Mishima, and K. Shiojima, *Jpn. J. Appl. Phys.*, **57**, 04FG13 (2018).
52. K. Isobe and M. Akazawa, *AIP Adv.*, **8**, 115011 (2018).
53. K. Isobe and M. Akazawa, *Jpn. J. Appl. Phys.*, **59**, 046506 (2020).